Binary tree models of high-Reynolds-number turbulence

Erik Aurell,[1,2] Emmanuel Dormy,[3,4] and Peter Frick[2,3,5]
[1]*Mathematics Department, Stockholm University, S-106 91 Stockholm, Sweden*
[2]*PDC/KTH, S-100 44 Stockholm, Sweden*
[3]*LMD/ENS, 24 rue Lhomond, F-75005 Paris, France*
[4]*IPG de Paris, 4 place Jussieu, F-75252 Paris Cedex 05, France*
[5]*Institute of Continuous Media Mechanics, Korolyov 1, 614061 Perm, Russia*
(Received 7 March 1997)

We consider hierarchical models for turbulence, that are simple generalizations of the standard Gledzer-Ohkitani-Yamada shell models (E. B. Gledzer, Dokl, Akad. Nauk SSSR **209**, 5 (1973) [Sov. Phys. Dokl. **18**, 216 (1973)]; M. Yamada and K. Ohkitani, J. Phys. Soc. Jpn. **56**, 4210 (1987)). The density of degrees of freedom is constant in wave-number space. Looking only at this behavior and at the quadratic invariants in the inviscid unforced limit, the models can be thought of as systems living naturally in one spatial dimension, but being qualitatively similar to hydrodynamics in two (2D) and three dimensions. We investigated cascade phenomena and intermittency in the different cases. We observed and studied a forward cascade of enstrophy in the 2D case. [S1063-651X(97)01708-X]

PACS number(s): 47.27.Eq

I. INTRODUCTION

The study of energy spectra and other statistical characteristics of fully developed turbulence in the inertial range now date back more than half a century [1]. Fully developed turbulence in the restricted sense is taken here to be the behavior of incompressible hydrodynamical flows at high Reynolds number, systems governed by the Navier-Stokes equations in three dimensions (3D). Partly by dimensional analogy, partly because direct numerical simulations are feasible, and partly because many physical flows are quasi-two-dimensional, although then properly described by more involved equations, it has become customary to also consider in parallel the more artificial case of the Navier-Stokes equations in two dimensions (2D) [2].

A long-standing problem in the 3D case is to determine if there are corrections to the classical prediction of Kolmogorov [3], which is traditionally derived from dimensional analysis and the physical picture of a cascade of energy down to small scales, where molecular diffusion is effective [4]. If all correlation functions are dominated by the same scaling behavior one would have

$$\langle (v(x+r)-v(x))^q \rangle \sim r^{\zeta_q} \tag{1}$$

with ζ_q equal to $q/3$. If different correlation functions are dominated by different scaling behaviors, ζ_q could be a rather arbitrary function of q, subject to the constraints that it is nondecreasing, its derivative is nonincreasing, and it passes through the points (0,0) and (3,1) [1].

The qualitative description of a cascade is generally considered to be correct. The experimental evidence leans towards the conclusion that there are corrections to the dimensional predictions, which are small for the spectrum, but larger for higher moments [5]. With a finite scaling range and experimental data that are never free from noise and other irregularities, the estimation of scaling exponents is always sensitive, especially for higher moments.

In 2D there is a second positive definite quadratic quantity, the enstrophy, which is inertially conserved. In analogy to the Kolmogorov theory in 3D one finds [6]

$$E(k) = C_\omega \epsilon_\omega^{2/3} k^{-3} \quad \text{Kraichnan's ``}k^{-3}\text{'' law,} \tag{2}$$

where ϵ_ω is the mean dissipation of enstrophy per unit time and mass, and C_ω is a dimensionless constant. Solutions to the 2D Euler equations are smooth for all times, and the energy spectrum can, therefore, never be flatter than Eq. (2). It could be steeper, but a spectrum decreasing as k^{-3} is a borderline case, in that if it is any steeper, the dominant interactions are no longer local in wave-number space. Enstrophy at small k would then jump directly to the dissipative range without an intermediate cascade from scale to scale. Most numerical experiments indicate significantly steeper spectra than the Kraichnan prediction [7]. The cascade picture is, therefore, probably qualitatively wrong for the 2D Navier-Stokes equations.

The density of degrees of freedom in a field problem in D dimensions grows with the wave number as

$$n(k) \sim k^{D-1}. \tag{3}$$

If the range of scales is from k_{small} to k_{large} the number of degrees of freedom is approximatively $(k_{\text{large}}/k_{\text{small}})^D$. When D is equal to 3 a range of scales of just 1000 is beyond the reach of present-day computers, and direct simulation of truly high-Reynolds-number turbulence will not be feasable in the foreseeable future. This is the motivation for considering various phenomenological models that share some of the properties of the full equations, but where the number of degrees of freedom is much less, and where much wider scaling ranges can be investigated.

In this paper we will investigate a class of such models where the density of degrees of freedom is constant, that is, they could be thought of as field problems in one dimension. In this sense they are intermediate between the full equa-

tions, or models where approximately the same number of degrees of freedom are kept, and shell models, which can be thought of as field problems in zero spatial dimensions. The outline of the paper is as follows: In Sec. II we describe shell models and other hierarchical models introduced in the literature. In Sec. III we introduce the models studied in this paper, and in Sec. IV we describe our numerical implementation and results. One of those, that in a naive first implementation all degrees of freedom in one shell synchronize, falls somewhat outside our main line of argument, and is discussed separately in Sec. V. In Sec. VI we summarize the discussion and conclude.

II. SHELL MODELS AND HIERARCHICAL MODELS

The basic idea of shell models is to describe with only one (or a few) variable U_N the velocity fluctuations in a wave-number octave ($2^N<|k|<2^{N+1}$). Different models, differing mainly in the number of variables per shell and the couplings were introduced by a number of authors [8–14].

The arguably simplest models are the ones introduced by Gledzer [10] and revived by Yamada and Ohkitani [13], now commonly referred to as the GOY model [15]. These consist in the following set of complex ordinary differential equations:

$$(d_t+\nu k_N^2)U_N=ik_N\left\{U_{N+1}^*U_{N+2}^*-\frac{\varepsilon}{2}U_{N-1}^*U_{N+1}^*-\frac{(1-\varepsilon)}{4}U_{N-2}^*U_{N-1}^*\right\}+f_N. \tag{4}$$

Here, * stands for conjugation, f_N a random force acting only on the few shells near $N=0$, and ε is a free parameter. The wave number k_N of the Nth shell is 2^N.

For any ε the GOY models conserve energy and phase space volume in the inviscid force-free limit, if these are defined in a natural way as

$$E=\sum_N |U_N|^2, \tag{5}$$

$$dV=dU_1^*\times dU_1\times\cdots. \tag{6}$$

If one makes the ansatz that a quadratic diagonal form is conserved

$$W=\sum_N |U_N|^2 z^N, \tag{7}$$

one finds that the variable z must satisfy a quadratic equation

$$(\varepsilon-1)z^2-\varepsilon z+1=0. \tag{8}$$

This equation admits two solution, $z=1$ and $z=1/(\varepsilon-1)$. The first solution corresponds to the energy conservation as above in Eq. (5), while the second gives another invariant

$$Z=\sum_N \mathrm{sgn}(\varepsilon-1)^N k_N^{\alpha(\varepsilon)}|U_N|^2,\quad \alpha(\varepsilon)=-\log_2(|\varepsilon-1|). \tag{9}$$

If ε is less than 1 the second invariant is indefinite like the helicity in 3D hydrodynamics, and it has the same dimensional form at the Yamada-Ohkitani value of ε equal to $\frac{1}{2}$ [16]. A large part of the phenomenology of turbulence was verified in this model in a series of papers [15–20], which stimulated the recent interest from several groups. A numerical study of the transition to chaos in the shell models with $0<\varepsilon<1$ was performed by Biferale *et al.* [21]. They found that there is a stable fixed point for $\varepsilon<\varepsilon_1=0.3843$, which goes unstable via a Hopf bifurcation, and above a larger value $\varepsilon_2=0.3953$, the system evolves into a chaotic state.

If, on the other hand, ε is greater than 1, the second invariant is a positive definite like the enstrophy in 2D hydrodynamics, and it has the same dimensional form as the physical enstrophy when ε is equal to $\frac{5}{4}$. In the interval between 1 and 2 the exponent α is positive and one naively expects a similar situation as in Kraichnan's model of 2D turbulence, i.e., a forward cascade of the second conserved quantity. At larger values than 2, the roles of the invariants change, and one expects a forward cascade of energy. At the boundary, ε is equal to 2 and the two invariants coincide: that would be a model of 3D turbulence without the helicity invariant.

In fact, shell models do not reproduce the forward cascade of enstrophy in 2D. It was shown in [22] that the GOY model at ε equal to $\frac{5}{4}$ is described by formal statistical mechanics, close to equilibrium. Enstrophy flows from the force to the dissipation, but in a process similar to heat flow in thermodynamics. This is not a cascade process, although some of the dimensional predictions fortuitously turn out to be correct. The simplest way to see this is that the resistance to transport increases with the distance between the scale, as the resistance to heat flow increases with the diffusing distance. This case implies that quantities in the inertial range depend on the viscosity parameter ν. The numerical results in [23] were confirmed in [24], and extended to the whole range of ε between 1 and 2.

The motivation for hierarchical models, in contrast to shell models, is that the growth of the number of degrees of freedom with the wave number is an important property of turbulence, and should be in some degree preserved. Such models were first introduced about the same time as shell models [25,11]. These models have in common that the number of degrees of freedom of the underlying system is kept, more or less: hence, 8^N variables in the Nth shell for hydrodynamics in 3D [11], and 4^N variables in the Nth shell for hydrodynamics in 2D [26,27]. The disadvantage of this approach is that the resulting equations become about as time consuming to simulate as the full hydrodynamic equations, although certainly the numerical code is much simpler. To get a model which has many degrees of freedom, but which is, nevertheless, significantly easier to simulate than the full equations one has to try an intermediate solution, as we describe below in Sec. III.

A second motivation is the above described discovery that the 2D GOY model does not display a forward cascade of enstropy. The theoretical explanation in [22] uses the observation that the characteristic times in the forward range of the transport of enstrophy are constant, and thus assumes that it is the increasing number of degrees of freedom in the full equations that drives the transport process preferably in the

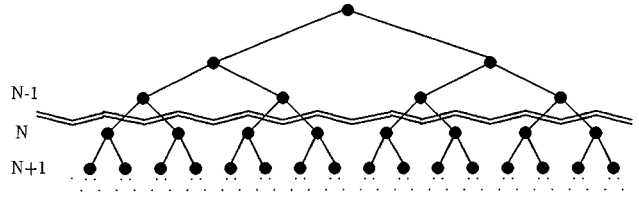

FIG. 1. Binary tree and convention for flux computations: the local energy (enstrophy) flux through a given node n in level N, is defined by all energy (enstrophy) exchanges with nodes on higher levels. The total flux through level N is the sum over n of the local fluxes.

direction of high wave numbers, that is, which leads to a cascade. Earlier investigations of a hierarchical tree model in [27], which could be considered a system of the type of 2D hydrodynamics in two spatial dimensions, did display such a cascade. It is therefore of some interest to see if this also happens in a system of the 2D hydrodynamical type in one spatial dimension.

III. BINARY MODEL

The first version of our model is a straightforward adaptation of the GOY model to a binary tree (Fig. 1).

We use N for notation of the number of the shell (the scale) and n for the individual number of variable inside the shell. We will also use a condensed notation for the variables when a computation is performed with N and n fixed, we omit to write n, if the meaning in this context is clear. For all terms written U_{N-1}, the suppressed index is such that this node is the parent of $U_{N,n}$. Similarly U_{N+1} stands for the children of $U_{N,n}$, usually with a summation implied. The equations of motion will then be identical to Eq. (4), and the conserved quantities will be completely analogous to Eqs. (5) and (9). In fact, we have mostly simulated a real version of Eq. (4) on a binary tree. The equations then read the same without the factor i and the complex conjugations on the right-hand side. All formulas below read the same for the real model, if the obvious substitutions are made.

The inertially conserved quantities are, in analogy with Eqs. (5) and (9),

$$E=\sum_{N,n} U_{N,n}^2 \tag{10}$$

and

$$Z_\alpha=\sum_{N,n} k_N^\alpha U_{N,n}^2. \tag{11}$$

The energy flux through one node can be defined as follows. Let us look at one particular node (N,n) and on all nodes in the binary tree subtended below it. Then

$$\frac{1}{2}\frac{d}{dt}\sum_{\text{below }(N,n)}|U_{N',n'}|^2=[\text{flow through }(N,n)]-[\text{viscous loss below }(N,n)]. \tag{12}$$

That gives

$$\Pi_E^{N,n}=k_N\left[\mathrm{Im}\langle U_N U_{N-1}U_{N-2}\rangle\left(\frac{\varepsilon-1}{4}\right)-\frac{1}{2}\,\mathrm{Im}\langle U_{N+1}U_N U_{N-1}\rangle\right], \tag{13}$$

where we have used the shorthand that U_N stands for the amplitude $U_{N,n}$, U_{N-1} and U_{N-2} for its parent and grandparent, respectively, and U_{N+1} for its two children. A summation over the children is implied. The total flux of energy through a shell is just Eq. (13) summed over all the nodes n in one layer.

Similarly, the enstrophy flux through a node (N,n) is

$$\Pi_Z^{N,n}=k_N^{1+\alpha}\left[\mathrm{Im}\langle U_N U_{N-1}U_{N-2}\rangle\left(\frac{\varepsilon-1}{4}\right)+\mathrm{Im}\langle U_{N+1}U_N U_{N-1}\rangle\left(1-\frac{\varepsilon}{2}\right)\right], \tag{14}$$

It turns out that this simple model, which we have just described, has the property that all the nodes in one level synchronize. The numerical evidence for this fact, which holds for using both complex and real amplitudes, and for all values of ε which we have investigated, is described below in Sec. IV. We do not quite understand why it happens. As it is somewhat accidental to our main purpose in this paper we have collected our remarks, as far as they go, separately in Sec. V. Let us just note here that if synchronization occurs, all the dynamically excited degrees of freedom in one layer can be represented by just the totally symmetrical combination $S_N=2^{-N}\Sigma_n U_{N,n}$. The equations of motion for the S_N's with different N will be precisely the original GOY equations (4).

A straightforward adaptation of the binary model that leads to interesting dynamics is to introduce dynamical couplings between neighboring nodes on one scale. This has some similarity with hydrodynamics, where vortices both interact with other close-by vortices of the same size and are advected and sheared by vortices of a larger size.

The most general GOY-like interaction term among neighboring nodes on one level is

$$AU_{N,n-2}U_{N,n-1}+BU_{N,n-1}U_{N,n+1}+CU_{N,n+1}U_{N,n+2}. \tag{15}$$

Conservation of energy, and of the second invariant, implies

$$A+B+C=0, \tag{16}$$

and for obvious symmetry reasons $A=C$. Using one overall parameter δ, which measures the strength of interactions between neighbors of the same scale, we have an additional piece in the equations of motion:

$$\delta(U_{N,n-2}U_{N,n-1}-2U_{N,n-1}U_{N,n+1}+U_{N,n+1}U_{N,n+2}). \tag{17}$$

For completeness we write here the equations finally proposed in the form that holds for real amplitudes

$$\left(\frac{d}{dt}+\nu k_N^2\right)U_{N,n}=k_N\Big[U_{N+1}U_{N+2}-\frac{\varepsilon}{2}\,U_{N-1}U_{N+1}$$
$$-\frac{(1-\varepsilon)}{4}\,U_{N-2}U_{N-1}+\delta(U_{N,n-2}U_{N,n-1}$$
$$-2U_{N,n-1}U_{N,n+1}+U_{N,n+1}U_{N,n+2})\Big]$$
$$+f_N. \tag{18}$$

To avoid boundary problems, that is a singular behavior of nodes on the edge of the tree, we impose a periodical condition. The tree could therefore be pictured to lie on the surface of a cone.

In an earlier paper of the two of the present authors [27], we motivated a hierachical tree model by writing the 2D Navier-Stokes' equations in a wavelet basis (cf. [28]). If we interpreted our binary model as a system of equations for the coefficients in a wavelet expansion of a field on the circle, we can go backwards, synthesize the field and write our model as an integral equation of the type

$$\partial_t u(x,t)=\nu\int K(x,x')u(x',t)$$
$$+\int I(x,x',x'')u(x',t)u(x'',t)+f(x,t). \tag{19}$$

The first kernel K is similar to a Laplacian as an integral operator, that is, to the second derivative of a δ function. The second kernel I collects the nonlinear interaction terms and inherits the symmetries of the GOY model. The details of both kernels, of course, depend on the choice of the wavelet basis we use to build the field. This analogy can perhaps be used to compare with the partial differential equation model in one dimension, but we will not pursue this question further here.

IV. NUMERICAL IMPLEMENTATION

A first implementation was done of the first naive model in the version with complex amplitudes and run on a work station. A second implementation was done on the massively parallel computer CM5 at Centre National de Calcul Parallèle en Sciences de la Terre (CNCPST) [29]. All results shown are from runs using this code. We simulated systems up to 18 level (131 071 nodes), using a 4th-order Runge-Kutta scheme for the integration.

We first present some results to illustrate the desynchronization of the tree by variation of parameter δ in Eq. (18). As measure of the ''desynchronization'' we use a quantity, defined as

$$\sigma=\frac{\Sigma(U_1-U_2)^2}{\Sigma U_i^2}, \tag{20}$$

where U_1 and U_2 describe all the pairs of the last level, and U_i all leaves of the last level. When the tree is fully synchronized, σ is zero. We studied the influence of parameter δ on the behavior of the system on a small model ($N=12$) with a fixed value of ε. In the 2D case ($\varepsilon=\frac{5}{4}$), we increased δ from 0.0 to 1.5 with step 0.5 (Fig. 2). As δ increases, the mean value of desynchronization increases, as well as the variance. In Fig. 3 we show the results for $\varepsilon=\frac{1}{2}$ when the variables in the last two shells were initialized to be zero.

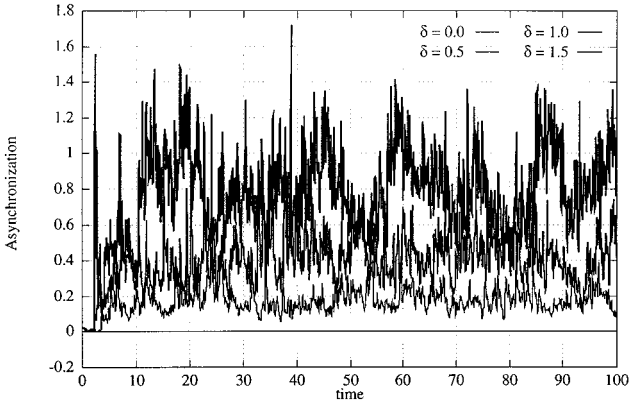

FIG. 2. Desynchronization in time in the model which includes interactions between the neighbors on one level and horizontal periodicity. $\varepsilon=\frac{5}{4}$, Reynolds number $\mathrm{Re}=5\times10^6$.

Figure 4 presents energy and enstrophy spectra, for a simulation of the 2D case, which should be compared with Kraichnan's ''k^{-3}'' law. One can see that there are very small, if any, deviations.

We also studied the higher structure functions, that we define by

$$S_p(N)=\sum_n \langle|U_{Nn}|^p\rangle \tag{21}$$

and we extract the scaling exponents in analogy with Eq. (1). To compute them with high accuracy we exploit the recent discovery of extended self-similarity in turbulence data [30], which means that if the moments are normalized by one of them, the scaling range and, thus, the accuracy of the determination of the scaling exponents of the quotient, can be significantly improved. Since in 3D, ζ_3 is asymptotically equal to one, it is customary to normalize by the third moment, i.e.,

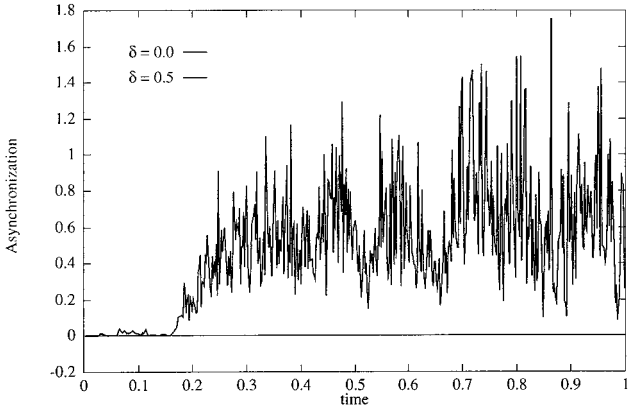

FIG. 3. Desynchronization in time for $\varepsilon=\frac{1}{2}$. One can observe that although the model is initialized with synchronized terminal leaves (the two last levels are set to zero) the systems dynamically desynchronizes. The Reynolds number here is 10^4, and the time step is 0.0002 for $\delta=0$, and 0.0001 for $\delta=0.5$.

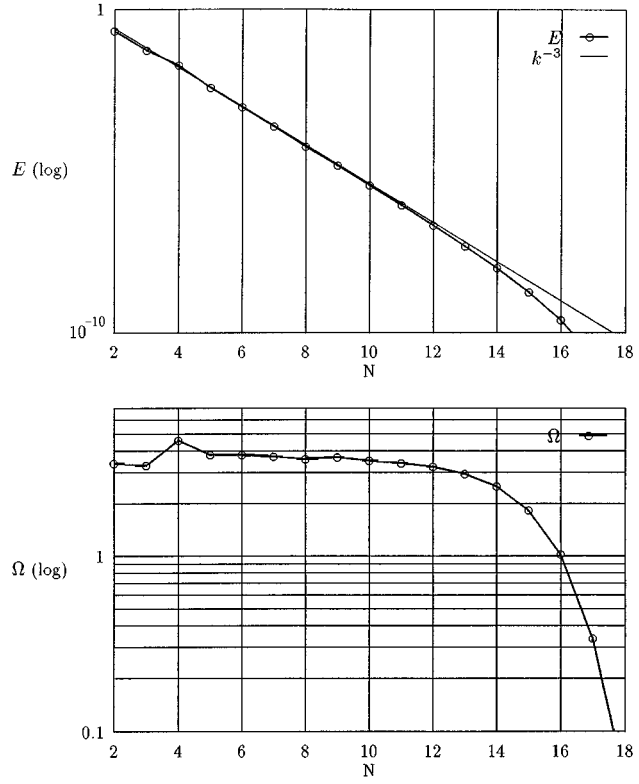

FIG. 4. Energy and enstrophy spectra for the 2D model, $\varepsilon=\frac{5}{4}$, and $\delta=1$. The number of levels was $N=18$. The Reynolds number was 1.0×10^{10}. The run time was 20 turn-over times.

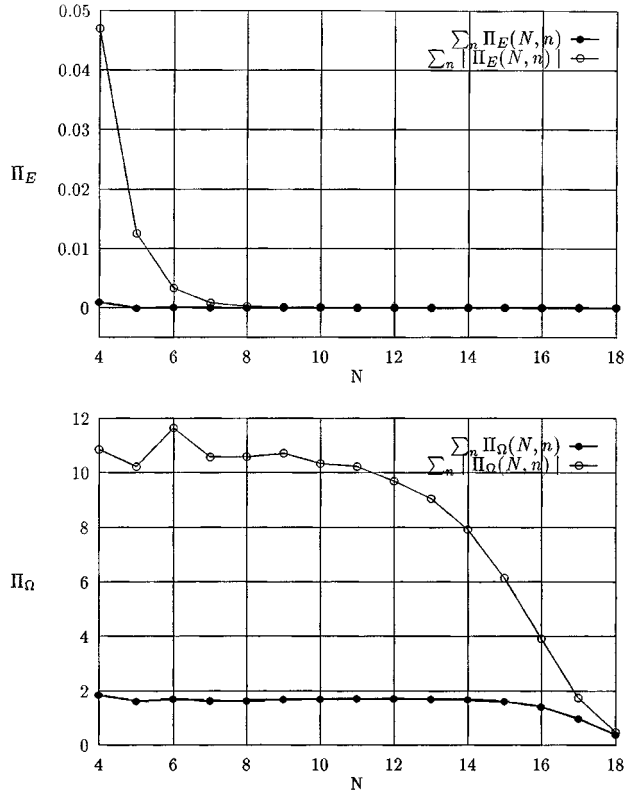

FIG. 5. Mean energy and enstrophy flux, same simulation as in Fig. 4.

$$\zeta_q=\zeta_3\tilde{\zeta}_q\,. \tag{22}$$

In 3D, ζ_q and $\tilde{\zeta}_q$ will be asymptotically equal, but a direct determination of $\tilde{\zeta}_q$ is expected to be more exact. In the 2D part lack of accuracy in the determinantion of any scaling exponent is instead collected in one overall factor ζ_3. The mean energy and enstrophy fluxes, level by level, are shown in Fig. 5. Our numerical values of the $\tilde{\zeta}_q$'s in the 2D case are shown in Fig. 6. It is clear that the energy flux is small, very close to zero, but that the enstrophy flux, or at least its fluctuations, is significant. Though not perfectly converged, the flux of enstrophy appears to be constant on about eight consecutive shells.

We also studied the case $\varepsilon=\frac{1}{2}$ which corresponds to the standard GOY model of 3D turbulence. Since the time step then depends on the size of the model, we tried, in this case only, systems up to $N=12$, and Reynolds number up to 2.0×10^3. The results are therefore at this stage preliminary, and will be presented in another context.

V. ON SYNCHRONIZATION

In the naive model without in-level couplings we observed synchronization of the different variable in one shell for different values of the model parameter ε. In particular, we observed this phenomenon both for the 2D case ($\varepsilon=\frac{5}{4}$), and the 3D case ($\varepsilon=\frac{1}{2}$) [29]. We cannot only explain this in part.

Suppose that the lowest level (the shell with the largest index) is M. Then, if synchronization is supposed to be important, it is resonable to take new variables which are the symmetric and antisymmetric combinations of the pairs of amplitudes on this last level. More formally, let

$$S_j^{M,1}=(U_{M,2j}+U_{M,2j+1}), \tag{23}$$

$$A_j^{M,1}=(U_{M,2j}-U_{M,2j+1}), \tag{24}$$

where $U_{M,2j}$ and $U_{M,2j+1}$ are two adjacent variables in the last level. Since they are siblings they share the same parent, which in this notation would be called $U_{M-1,j}$, and the grandparent, and so on.

The equations of motion of the symmetrized and antisymmetrized combinations are

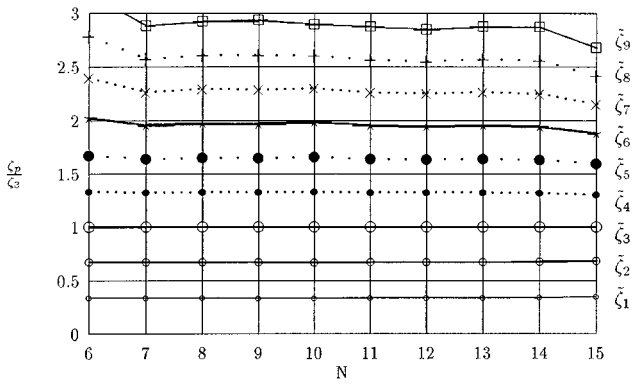

FIG. 6. The relative scale exponents $\tilde{\zeta}_p$ (following the extended self-similarity), for the $2D$ model, $\varepsilon=\frac{5}{4}$ and $\delta=1$. We can see that there are but very small, if any, effects of space-time intermittency.

$$(d_t+\nu k_M^2)A_j^{M,1}=0, \tag{25}$$

$$(d_t+\nu k_M^2)S_j^{M,1}=ik_M\left\{-\frac{(1-\varepsilon)}{4}\,U_{M-2}^*U_{M-1}^*\right\}. \tag{26}$$

It follows of course that the antisymmetrized combinations at the last level die out, that is, that siblings on the lowest level synchronize.

It is tempting to assume that this behavior holds for higher and higher levels, such that eventually the whole tree gets synchronized. We cannot, however, make such an argument work, because at higher levels the equations of motion for the symmetrized and antisymmetrized combinations do not decouple.

To see this effect it is sufficient to look at the next two levels, which is still a situation a little easier to see than in the middle of the tree. Let us take a subtree hanging on one of the nodes on level $M-2$ and call that $U_{M-2,j}$. We assume that the pairs on the lowest level have synchronized, as we know they must, and there are then four (not six) dynamic variables on the branches of the tree hanging below, namely, $U_{M-1,2j}$, $S_{2j}^{M,1}$, $U_{M-1,2j+1}$, and $S_{2j+1}^{M,1}$. Again, if symmetrization is assumed to be important in this subtree, it is reasonable to introduce the symmetric and antisymmetric combinations as follows:

$$S_j^{M-1,1}=(U_{M-1,2j}+U_{M-1,2j+1}), \tag{27}$$

$$A_j^{M-1,1}=(U_{M-1,2j}-U_{M-1,2j+1}), \tag{28}$$

$$S_j^{M,2}=(S_{2j}^{M,1}+S_{2j+1}^{M,1}), \tag{29}$$

$$A_j^{M,2}=(S_{2j}^{M,1}-S_{2j+1}^{M,1}). \tag{30}$$

Writing the equations of motion for these variables we have

$$(d_t+\nu k_M^2)A_j^{M,2}=ik_M\left\{-\frac{(1-\varepsilon)}{4}\,U_{M-2,j}^*(A_j^{M-1,1})^*\right\}, \tag{31}$$

$$(d_t+\nu k_{M-1}^2)A_j^{M-1,1}=ik_{M-1}\left\{-\frac{\varepsilon}{2}\,U_{M-2,j}^*(A_j^{M,2})^*\right\}, \tag{32}$$

$$(d_t+\nu k_M^2)S_j^{M,2}=ik_M\left\{-\frac{(1-\varepsilon)}{4}\,U_{M-2}^*(S_j^{M-1,1})^*\right\}, \tag{33}$$

$$(d_t+\nu k_{M-1}^2)S_j^{M-1,1}=ik_M\left\{-\frac{\varepsilon}{2}\,U_{M-2}^*(S_j^{M,2})^*, \right. \tag{34}$$

$$\left.-\frac{(1-\varepsilon)}{4}\,U_{M-3}^*U_{M-2}^*\right\}. \tag{35}$$

We see that the equations are linear in the A's and that the A's do not act back on the S's. Under reasonable assumptions on the off-diagonal driving terms, that is, in this case $U_{M-2,j}^*$, it would still follow that eventually the two coupled antisymmetrized combinations die out. If we look at higher levels we will, however, eventually find that quadratic combinations of antisymmetrized combinations act back and drive the symmetrized combinations. To show that the last two levels synchronize is thus as far as we get.

By a more qualitative argument we can, however, make it very plausible that synchronization occurs. Take the two subtrees hanging on one of the nodes on level N, where N is far up in the tree, and assume that both trees are completely synchronized. Their dynamical degrees of freedom are then the remaining symmetrized combinations, that we call $(x_{N+1},\ldots,x_M)$ and $(y_{N+1},\ldots,y_M)$ for short. The equations of motion for $\vec{x}$ can be written

$$d_t x_{N+1}=F_{N+1}(\vec{x})+x_{N+2}G_N, \tag{36}$$

$$d_t x_{N+2}=F_{N+2}(\vec{x})+x_{N+1}H_N, \tag{37}$$

$$d_t x_{N+i}=F_{N+i}(\vec{x})N+3\leqslant i\leqslant M, \tag{38}$$

where the F's give the couplings of the x variables between themselves, and G and H give the coupling through the top node (N,n). The equations for $\vec{y}$ are completely similar. The two equations are not uncoupled, because they are both driven by the variables G_N and H_N, which in turn are driven by the symmetric combinations of (x_{N+1},y_{N+1}) and (x_{N+2},y_{N+2}), respectively. We therefore appeal to Huygen's principle, that identical nonlinear coupled oscillators tend to lock in phase. We believe this is what happens. It is true that Huygen's principle is generally applied to periodic oscillators, and we have here *de facto* two chaotic oscillators, which is a weakness of the argument just presented.

VI. CONCLUSION

We have presented a simplified hierachical model of turbulence, which can be looked upon as the GOY shell models on a binary tree. The model is easy to simulate and allows us to investigate cascade processes in a much wider range of scales than in previously introduced hierarchical models, or in the full equations. A first naive implementation leads to synchronization of the dynamical degrees of freedom on one scale. One simple additional interlevel coupling term breaks this effect.

We investigated intermittency corrections to the Kolmogorov and Kraichnan predictions. As in shell models, a cascade process would lead to the same spectral behavior as in the full equation, that is $E(k)\simeq k^{-3}$ in the Kraichnan theory. An equilibrium situation does however, simply by considering the density of degrees of freedom, lead to $E(k)\simeq k^{D-3}$ in the forward enstrophy transport range [2]. For the full 2D Navier-Stokes equations this is $E(k)\simeq k^{-1}$, while for the 2D shell models it is $E(k)\simeq k^{-3}$, i.e., by coincidence the same as the cascade prediction. In our model we have the intermediate law $E(k)\simeq k^{-2}$. Since we observe a behavior very close to $E(k)\simeq k^{-3}$ a cascade picture can be established already from the spectrum.

ACKNOWLEDGMENTS

E.A. thanks Laboratoire Physico-Chémique Théorique at ESPCI (Paris) for hospitality. P.F. thanks the Center for Parallel Computers for hospitality. E.D. and P.F. thank the CNCPST for use of the CM5 and the Laboratory of Dynami-

cal Meteorologie (Paris) for hospitality. This work was supported by the Swedish Natural Science Research Council through Grant No. S-FO 1778-302 (E.A.), by the French Ministry of Superior Education and Research (MESR) through free access to the CM-5, and by the Swedish Royal Academy of Sciences. We thank Claude Basdevant and Luca Biferale for discussions. E.D. thanks Dmitri Pissarenko for useful discussions.

[1] U. Frisch, Proc. R. Soc. London, Ser. A **434**, 89 (1991); U. Frisch, Turbulence: The Legacy of A. N. Kolmogorov (Cambridge University Press, Cambridge, 1995).
[2] R. H. Kraichnan, and D. Montgomery, Rep. Prog. Phys. **43**, 547 (1980).
[3] A. N. Kolmogorov, Dokl. Akad. Nauk SSSR, **30**, 301 (1941) [Sov. Phys. Dokl. **30**, 4 (1941)].
[4] L. Landau and E. Lifshitz, *Course on Theoretical Physics: Volume 6 Hydrodynamics* (Pergamon, New York, 1987).
[5] Y. Gagne and B. Castaing, C.R. Acad. Sci. Paris **312**, 414, (1991); F. Anselmet, Y. Gagne, E. J. Hopfinger, and R. A. Antonia, J. Fluid Mech. **140**, 63 (1984).
[6] R. H. Kraichnan, J. Fluid Mech. **47**, 525 (1971).
[7] U. Frisch and P. Sulem, Phys. Fluids **27**, 1921 (1984).
[8] A. M. Obukhov, Atmos. Oceanic Phys. **7**, 41 (1971).
[9] V. N. Desnjanskii and E. A. Novikov, J. Appl. Math. Mech. **38**, 468 (1972).
[10] E. B. Gledzer, Dokl. Akad. Nauk SSSR **209**, 5 (1973) [Sov. Phys. Dokl. **18**, 216 (1973)].
[11] V. D. Zimin, Izv. Akad. Nauk. SSSR, Fiz. Atm. Okeana **17**, 941 (1981).
[12] P. G. Frick, Magnetohydrodynamics **19**, 48 (1983).
[13] M. Yamada and K. Ohkitani, J. Phys. Soc. Jpn. **56**, 4210 (1987).
[14] J. Eggers and S. Grossman, Phys. Lett. A **156**, 444 (1991).
[15] D. Pissarenko, L. Biferale, D. Courvoisier, U. Frisch, and M. Vergassola, Phys. Fluids A **5**, 2533 (1993).
[16] L. Kadanoff, D. Lohse, J. Wang, and R. Benzi, Phys. Fluids **7**, 617 (1995).
[17] L. Biferale and R. Kerr, Phys. Rev. E **52**, 6113 (1995).
[18] R. Benzi, L. Biferale, R. Kerr, and E. Trovatore, Phys. Rev. E **53**, 3541 (1996).
[19] A. Crisanti, M. H. Jensen, G. Paladin, and A. Vulpiani, Phys. Rev. Lett. **70**, 166 (1993); J. Phys. A **26**, 6943 (1993).
[20] M. H. Jensen, G. Paladin, and A. Vulpiani, Phys. Rev. A **43**, 798 (1991); **45**, 7214 (1994).
[21] L. Biferale, A. Lambert, R. Lima, and G. Paladin, Physica D **80**, 105 (1995).
[22] E. Aurell, G. Boffetta, A. Crisanti, P. Frick, G. Paladin, and A. Vulpiani, Phys. Rev. E **50**, 4705 (1994).
[23] E. Aurell, G. Boffetta, A. Crisanti, G. Paladin, and A. Vulpiani, Phys. Rev. E **53**, 2337 (1996).
[24] P. D. Ditlevsen and I. A. Morgensen, Phys. Rev. E **53**, 4785 (1996).
[25] E. D. Siggia, Phys. Rev. A **15**, 1730 (1977); **17**, 1166 (1978).
[26] A. B. Mikishev and P. G. Frick, Magnetohydrodynamics **25**, 127 (1989).
[27] E. Aurell, P. Frick, and V. Shaidurov, Physica D **72**, 95 (1994).
[28] M. Holschneider, Wavelets: An Analysis Tool (Clarendon, Oxford, 1995).
[29] E. Dormy (unpublished).
[30] R. Benzi, S. Ciliberto, C. Baudet, G. Ruiz, and R. Tripiccione, Europhys. Lett. **24**, 275 (1993).